

Short Communication

Effect of Superabsorbent Polymer as Partial Replacement of Portland Cement on Electrochemical Corrosion Behavior of Carbon Steel Rebar in Artificial Seawater

Baoqing Zhang^{1,2}

¹ School of Water & Architectural Engineering, Shihezi University, Shihezi 832000, China

² School of Architecture and Urban planning, Huazhong University of Science and Technology, Wuhan Hubei 430047 China

E-mail: baqingzhang86@sina.com and D201677799@hust.edu.cn

Received: 31 December 2020 / Accepted: 2 February 2021 / Published: 28 February 2021

The effect of superabsorbent polymer (SAP) powder and fly ash (FA) content into concrete structures on the corrosion behavior of carbon steel rebar was studied. SAPs were applied at various volume fractions (0.1%, 0.2%, and 0.4%). All the SAP-modified concrete samples contained 15wt% FA as a cement replacement. The electrochemical analysis was done by electrochemical impedance spectroscopy (EIS) and polarization measurement assessments in 3.5wt% NaCl as artificial seawater. The EIS results fitted by an appropriate equivalent electrical circuit indicated that the highest corrosion resistance was achieved for the SAP4 mixture. Polarization analysis revealed that the SAP4 sample has the lowest corrosion current density, more positive corrosion potential with high corrosion protection. These electrochemical results show that the simultaneous addition of FA and SAPs admixtures in concrete structures improve the concrete durability and corrosion resistance of carbon steel rebar after being exposed to an aggressive environment by preventing the rebar surface from reaching the corrosive ions.

Keywords: Superabsorbent polymer powder; Fly ash admixture; Carbon steel reinforced concrete; Electrochemical corrosion behavior

1. INTRODUCTION

The corrosion in steel reinforced concrete decreases the durability and stability of concrete structure [1, 2]. Corrosion occurs due to the penetration of corrosive ions or loss of alkalinity of concrete [3]. Corrosion control techniques include surface treatments of steel rebars, the using partial replacement in Portland cement (PC), and cathodic protection [4]. Additives are independently attractive because they are reasonably inexpensive. The concrete quality can be enhanced by adding

various mineral additives such as Palm Oil Fuel Ash, fly Ash, Silica Fume, metakaolin and Rice Husk Ash [5]. Mineral admixtures affect the hardening properties of concrete [6, 7].

Polymers have been used in concrete structure to develop engineering characteristics such as enhancing durable properties of concrete, improving the compressive strength, increasing corrosion resistance and reducing the cracks extension [8]. Therefore, superabsorbent polymer (SAPs) can be applied for stated properties. Permeability may be decreased by addition of the polymer fibers [9]. One of the important parameters for making reinforced concrete and increasing the durability of concrete is crack width control [10, 11]. In particular, unexpected cracks formed due to the steel corrosion reduce the service life of reinforced concrete. The previous studies are mostly based on corrosion behavior of cement containing by-product materials and SAPs separately and the performance of such additives along with SAPs has not been well investigated especially, the effect of bagasse ash and SAPs [12-14].

In this study, different admixtures were manufactured to explore the effect of fly ash and SAPs in the concrete on the corrosion protection of embedded carbon steel rebar. A reinforced concrete made with a PC was used as a control sample. The corrosion behavior of samples was studied in artificial seawater using open circuit potential (OCP), polarization and electrochemical impedance spectroscopy (EIS) techniques for four weeks. Morphological property of samples was considered using scanning electron microscopy (SEM).

2. MATERIALS AND METHOD

The chemical compositions of PC and fly ash (FA) are shown in Table 1. Also the properties of SAPs are summarized in Table 2. FA was added as a PC replacement for 15 wt% by weight of cement. Moreover, different mixtures containing FA and various volume fractions of SAPs (0.1, 0.2, and 0.4%) were produced. For concrete casting, the mixing ratio of PC with water was 0.45. The mixture design is shown in Table 3. To produce uniform polymer-modified concrete, the mixed cements were blended by a high-speed mixer. For each measurement, three samples were prepared and the average value as the final result was shown.

Table 1. Chemical composition of Portland cement and Fly ash (% by mass)

Composition	Materials	
	Portland cement	Fly ash
SiO ₂	19.99	64.53
Fe ₂ O ₃	3.01	5.68
Al ₂ O ₃	4.78	25.79
CaO	63.49	0.58
MgO	2.01	0.26
K ₂ O	0.68	0.043
Na ₂ O	0.30	0.027
SO ₃	2.65	0.32
L.O.I	3.09	2.77

The concrete samples were poured into the cylindrical molds with a diameter of 10 cm and a height of 30 cm for 24 h at 95% relative humidity and room temperature to complete the hydration reaction.

Table 2. Properties of SAP particles

Dimension(μm)	80~120
Density (kg/m^3)	700
Water absorbing capacity -(g/g)	350
NaCl solution -(g/g)	45

Table 3. Compositions of prepared mixtures

Mixtures	Cement (kg/m^3)	Water (kg/m^3)	Fly ash (kg/m^3)	Fine aggregates (kg/m^3)	Coarse aggregates (kg/m^3)	Volume fraction of SAPs
PC	500	225	---	845	867	---
FA	425	225	75	838	863	---
SAP1	425	225	75	835	864	0.1
SAP2	425	225	75	832	861	0.2
SAP4	425	225	75	830	859	0.4

A carbon steel rebar was located vertically in the center of the cylinder. In this work, carbon steel with 8mm diameter was used to study the corrosion behavior of steel rebar in seawater solution. Table 4 indicates the chemical composition of used carbon steel.

Table 4. Chemical composition of used carbon steel (wt%)

C	Si	Mn	P	S	Fe
0.21	0.55	1.52	0.03	0.024	Residual

The steel rebars were polished and cleaned through SiC papers. All rebars were deep into the acetone solution and washed via DI water. Figure 1 shows a schematic diagram and detailed dimensions for a reinforced concrete sample.

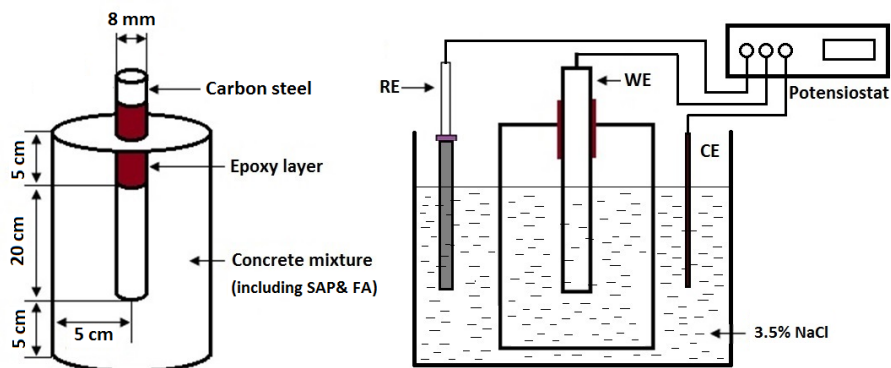


Figure 1. Schematic diagram of the carbon steel reinforced concrete used as a working electrode in electrochemical experiments

OCP were done by a high-input impedance voltmeter for the various systems. Polarization resistance and EIS as nondestructive monitoring techniques were applied to study the corrosion behavior of carbon steel rebars. A triple-electrode system was applied for the measurements which contain the steel bar embedded in concrete as the working electrode, a platinum wire and a saturated calomel electrode as an auxiliary and a reference electrode, respectively. The analysis was performed after immersed to 3.5wt% NaCl solution as artificial seawater. The EIS assessments were done at a frequency range from 0.01 Hz to 0.1 MHz after one month immersion time. The polarization analysis was done from 350 mV at a scan rate of 1 mV/s. The surface morphologies of the steel rebars were considered by scanning electron microscope (SEM, Zeiss Sigma 300 VP).

3. RESULTS AND DISCUSSION

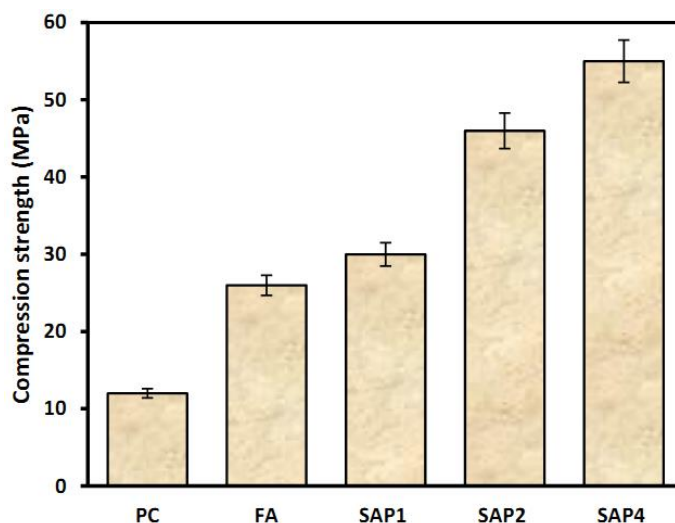


Figure 2. Compression strength of different specimens after four weeks of curing at room temperature

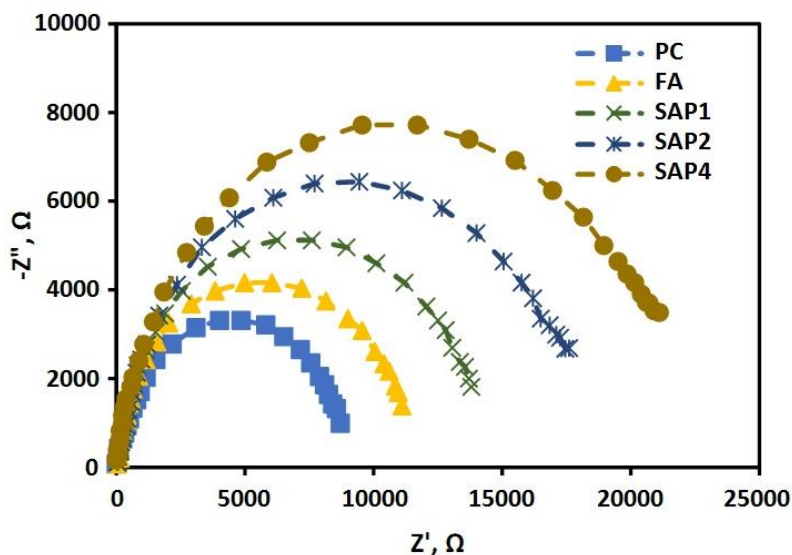


Figure 3. Nyquist plots of carbon steel reinforced concrete exposed to 3.5wt% NaCl solution at a frequency range from 0.01 Hz to 0.1MHz after one month immersion time

The compression strength results achieved for different specimens after four weeks of curing is revealed in figure 2. As shown, the mixture containing 0.4% SAPs had superior compression strength than the other specimens which was higher than the PC sample. The enhancement in compression strength for SAP4 sample can be related to the use of FA as a micro-filler in improving concrete structure. Furthermore, the FA as an activator is involved in the pozzolanic reaction which makes a denser structure and accelerates the hydration procedure, enhancing the compression strength [15]. Moreover, the increasing concentration of SAPs enhances the compression strength of concrete which can be an alternative technique to increase the durability of structure.

EIS method was used to assess the corrosion behavior of carbon steel rebar reinforced into the concrete with different additives in 3.5wt% NaCl solution. Figure 3 shows the Nyquist diagrams obtained by the EIS analysis. An equivalent circuit applied to fit the EIS result is indicated in Figure 4. Where R_s is the resistance of solution. R_f and C_f reveal the resistance and capacitance of coated concrete, respectively. R_{ct} and C_{dl} present the charge transfer resistance and double-layer capacitance of carbon steel bar surface, respectively [16]. The obtained data are summarized in table5.

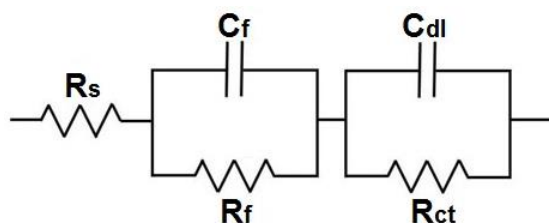


Figure 4. An equivalent circuit

Table 5. Achieved electrochemical parameters of fitting the Nyquist diagrams with an equivalent circuit

Mixture	R_s (Ω)	R_f (Ω)	$C_f(\mu F\ cm^{-2})$	R_{ct} (Ω)	$C_{dl}(\mu F\ cm^{-2})$
PC	47	5823	3.73	8650	5.21
FA	33	8749	2.68	12105	4.83
SAP1	54	11242	2.26	14860	4.17
SAP2	45	14873	1.97	18948	3.76
SAP4	58	20146	1.14	23597	2.75

These findings show that by the appropriate replacement of SAPs and FA in the PC, R_f increases and C_f reduces, which exhibits an enhancement in the stability for passive layer and corrosion resistance of the carbon steel bar [17]. Because of the high surface area of FA, it can create a robust adhesion to hydrated cement which helps to inhibit the better growth of $Ca(OH)_2$ [18]. The admixtures fill capillary pores and small cracks and finally shrink the cement structure which improves the corrosion behavior of steel bars in a corrosive environment. Furthermore, comparing C_{dl} and C_f , it was observed that C_f was lower than C_{dl} in all concrete samples which had confirmed that the creation of passive and double layers in the interfaces has high capacitive behavior [19].

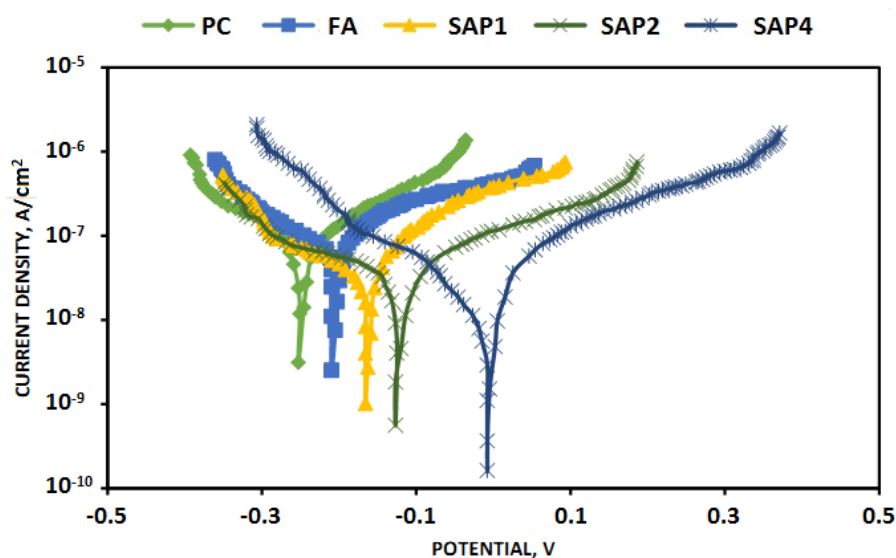


Figure 5. Polarization curves of carbon steel reinforced concrete specimens with different content of admixtures exposed to 3.5% NaCl solution after one month exposure time at scan rate of 1 mV/s

The polarization curves of carbon steel reinforced concrete specimens exposed to 3.5wt% NaCl solution for four weeks are shown in Figure 5 to assess the effect of SAPs content on corrosion behavior of carbon steel bars. The values of corrosion potential and corrosion current density are indicated in table 6 which are attained from the polarization plots in Figure 5. The concrete specimen

without admixtures had the lowest corrosion potential than the other concrete samples. The steel reinforced concrete specimen with 0.4% SAPs was at a passive state and had fewer tendencies to corrosion. As revealed in figure 5, increasing SAPs content leads to a considerable increase in the corrosion potential (E_{corr}). Hence, the potential had moved to more positive value. Moreover, corrosion current density (I_{corr}) shifted to the left side which revealed that there is less corrosion current on the carbon steel rebar surface [20]. The corrosion level can be divided in four levels stated by the Durar-Network Specification [21]. However, the I_{corr} of SAP4 sample in artificial seawater was lower compared to the other samples (Table 6). Therefore, except the PC sample, all carbon steel rebars stayed at the passive state during the electrochemical process which indicated their great corrosion resistance of carbon steel rebars into 3.5wt% NaCl solution.

Table 6. Corrosion potential and corrosion current density of carbon steel rebars

Admixture	Corrosion current density ($\mu\text{A}/\text{cm}^2$)	Corrosion potential (V)
PC	0.121	-0.255
FA	0.098	-0.209
SAP1	0.074	-0.154
SAP2	0.062	-0.127
SAP4	0.054	-0.033

The SAPs concentration has direct effect on the permeability of concrete and lower permeability causes the denser concrete structure [22]. Therefore, fewer corrosive ions were allowed to come in the concrete structures. Thus, the I_{corr} can be less and E_{corr} can be more positive. The corrosion of carbon steel rebar in concrete samples with 0.4% SAPs was intensely reduced after four-week exposure to the 3.5wt% NaCl media which had more corrosion resistance than the other concretes. It can be related to the amount of SAPs which had a direct influence on the reinforced concrete performance.

The OCP is a recognized technique to determine the corrosion resistance by the half-cell potential method. Figure 6 shows the results of OCP values of the carbon steel rebar reinforced in different concrete mixes exposed to the 3.5wt% NaCl solution for 4 weeks. In this process, the changes in potential between a reference electrode and steel rebar reinforced into concrete is considered consistent with ASTM C-876 [17, 23, 24]. Therefore, the potential values less than -0.350V are in the high-risk region, the ones between -0.200V and -0.350V are in the intermediate corrosion-risk region and the potential value more than -0.200V is in the low-risk region. As shown in Figure 6, the potential values of mixtures shift to a more positive value of E_{corr} with addition of FA and increase the volume fraction of SAPs which indicate less corrosion probability. Moreover, the SAP4 mixture reveals the most positive potential value among all SAP-reinforced fly ash concretes. The corrosion protection can be attributed to significant influence on the concrete durability enhancement due to the change in pores and reduction in calcium hydroxide [25]. Moreover, lower permeability and less penetration of corrosive ions can lead to the postponing corrosion and more durability of concrete structures [26].

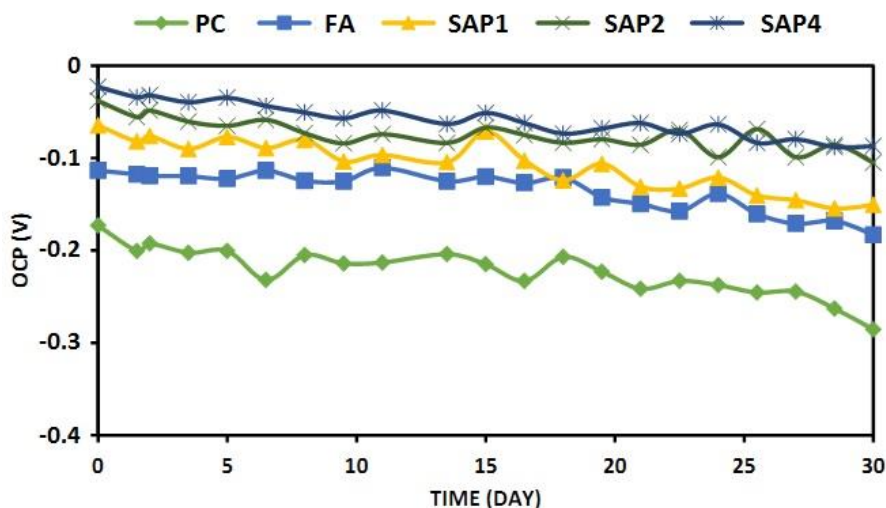


Figure 6. OCP values of the carbon steel rebar reinforced in various concrete mixes containing FA and different volume fractions of SAPs exposed to 3.5% NaCl at different immersion time

Figure 7 reveals the surface morphologies of the carbon steel rebar in PC without additional materials, FA mix and SAP4 mixture exposed to 3.5wt% NaCl solution after 4 weeks. When FA is added, the separation and irregularity of structures are observed. Fig. 7b exhibited that the sample with 15 wt% FA is more uniform and smooth than the PC mix which agrees with previous reports [27]. Figure 7c shows low pitting corrosion on the carbon steel surface. SAPs create the bridging effect which can increase the flexural and tensile strength. Furthermore, the SAPs include C-S-H gels and aggregates as binders can have the pore blocking effects leading to less permeability. Actually, by reducing the internal conductivity of the pores, it shows less capillary porosity [28].

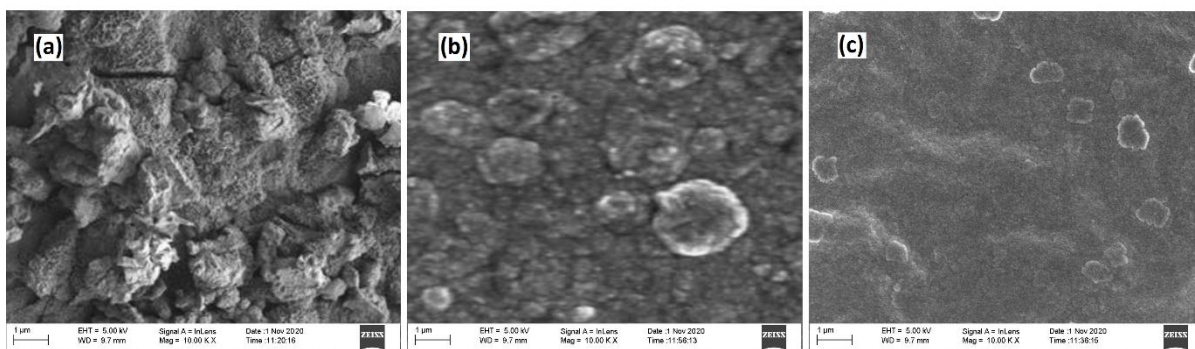


Figure 7. Surface morphologies of carbon steel in various concrete (a) PC mixture, (b) FA mixture and (c) SAP4 mixture exposed to the 3.5wt% NaCl solution for 4 weeks.

4. CONCLUSIONS

The effect of FA and SAPs content into concrete structures on the corrosion behavior of carbon steel rebar was investigated. SAPs were applied at various volumes. All the SAP-reinforced concrete

samples contained 15wt% FA as a cement replacement. The electrochemical analysis was done by EIS and polarization measurement assessments in 3.5wt% NaCl as artificial seawater. The EIS results fitted by an appropriate equivalent electrical circuit revealed that the highest corrosion resistance was achieved for the SAP mixture. Polarization analysis indicated that the SAP4 sample has the lowest corrosion density, more positive corrosion potential with high corrosion protection. These electrochemical results and water absorption show that the simultaneous addition of FA and SAPs admixtures in concrete structures improves the concrete durability and corrosion resistance of carbon steel rebar after being exposed to an aggressive environment by preventing the rebar surface from reaching the corrosive ions. Surface morphologies of carbon steel rebar indicated lower pitting corrosion on the SAP4 sample compared to the other samples which were in agreement with the electrochemical results.

References

1. V. Marcos-Meson, G. Fischer, C. Edvardsen, T.L. Skovhus and A. Michel, *Construction and Building Materials*, 200 (2019) 490.
2. S. Kakooei, H.M. Akil, M. Jamshidi and J. Rouhi, *Construction and Building Materials*, 27 (2012) 73.
3. S. Cheng, Z. Shui, X. Gao, J. Lu, T. Sun and R. Yu, *Cement and Concrete Composites*, 15 (2020) 103629.
4. X. Lv, *International Journal of Electrochemical Science*, 15 (2020) 7754.
5. M. Amin, B.A. Tayeh and I.S. Agwa, *Journal of Cleaner Production*, 273 (2020) 123073.
6. S. Elshafie, M. Boulbibane and G. Whittleston, *Construction Science*, 19 (2016) 4.
7. H. Karimi-Maleh, Y. Orooji, A. Ayati, S. Qanbari, B. Tanhaei, F. Karimi, M. Alizadeh, J. Rouhi, L. Fu and M. Sillanpää, *Journal of Molecular Liquids*, (2020) 115062.
8. A. Siddika, M.A. Al Mamun, R. Alyousef and Y.M. Amran, *Journal of Building Engineering*, 25 (2019) 100798.
9. S. Gupta, H.W. Kua and S.D. Pang, *Magazine of Concrete Research*, 70 (2018) 350.
10. A. Baricevic, M. Pezer, M.J. Rukavina, M. Serdar and N. Stirmer, *Construction and Building Materials*, 176 (2018) 135.
11. H. Karimi-Maleh, M. Alizadeh, Y. Orooji, F. Karimi, M. Baghayeri, J. Rouhi, S. Tajik, H. Beitollahi, S. Agarwal and V.K. Gupta, *Industrial & Engineering Chemistry Research*, 60 (2021) 816.
12. I. Curosu, M. Liebscher, V. Mechtcherine, C. Bellmann and S. Michel, *Cement and Concrete Research*, 98 (2017) 71.
13. D.-Y. Yoo and M.-J. Kim, *Construction and Building Materials*, 209 (2019) 354.
14. R. Mohamed, J. Rouhi, M.F. Malek and A.S. Ismail, *International Journal of Electrochemical Science*, 11 (2016) 2197.
15. P. Duan, Z. Shui, W. Chen and C. Shen, *Journal of Materials Research and Technology*, 2 (2013) 52.
16. S.B. Aoun, M. Bouklah, K. Khaled and B. Hammouti, *International Journal of Electrochemical Science*, 11 (2016) 7343.
17. S. Kakooei, H.M. Akil, A. Dolati and J. Rouhi, *Construction and Building Materials*, 35 (2012) 564.
18. Q. Wang, S. Li, S. Pan, X. Cui, D.J. Corr and S.P. Shah, *Construction and Building Materials*, 198 (2019) 106.

19. K. Sarkar, A. Mondal, A. Chakraborty, M. Sanbui, N. Rani and M. Dutta, *Surface and Coatings Technology*, 348 (2018) 64.
20. J. Shi, W. Sun, J. Jiang and Y. Zhang, *Construction and Building Materials*, 111 (2016) 805.
21. W. Zhao, J. Zhao, S. Zhang and J. Yang, *International Journal of Electrochemical Science* 14 (2019) 8039.
22. K. Tan and J. Zhu, *Materials and Structures*, 50 (2017) 56.
23. B. Assouli, G. Ballivy and P. Rivard, *Corrosion Engineering, Science and Technology*, 43 (2008) 93.
24. A.H.J. Al-Tayyib, M. Mesfer and A. Zahrani, *Materials Journal*, 87 (1990) 108.
25. P. Rattanachu, W. Tangchirapat and C. Jaturapitakkul, *Journal of Materials in Civil Engineering*, 31 (2019) 04019093.
26. A. Ramezani pour, M. Esmaeili, S.-A. Ghahari and M. Najafi, *Construction and Building Materials*, 44 (2013) 411.
27. V.A. Franco-Luján, M.A. Maldonado-García, J.M. Mendoza-Rangel and P. Montes-García, *Construction and Building Materials*, 198 (2019) 608.
28. V. Afroughsabet and T. Ozbakkaloglu, *Construction and building materials*, 94 (2015) 73.

© 2021 The Authors. Published by ESG (www.electrochemsci.org). This article is an open access article distributed under the terms and conditions of the Creative Commons Attribution license (<http://creativecommons.org/licenses/by/4.0/>).